

Electric-Field Effect on the Angle-Dependent Magnetotransport Properties of Quasi-One-Dimensional Conductors

K. Kobayashi,* M. Saito, E. Ohmichi, and T. Osada

Institute for Solid State Physics, University of Tokyo, 5-1-5 Kashiwanoha, Kashiwa, Chiba 277-8581, Japan

(Received 23 April 2004; published 30 March 2006)

We report a novel electric field effect on angular dependent magnetotransport in quasi-one-dimensional layered conductors with a pair of sheetlike Fermi surfaces. Under tilted magnetic fields and additional interlayer electric fields, semiclassical electron orbits on two Fermi sheets become periodic at different magnetic field orientations. This causes double splitting of the Lebed's commensurability resonance in interlayer transport, and the amount of splitting allows us to estimate the Fermi velocity directly. We have successfully demonstrated this effect in the organic conductor α -(BEDT-TTF)₂KHg(SCN)₄.

DOI: 10.1103/PhysRevLett.96.126601

PACS numbers: 72.15.Gd, 72.80.Le, 73.21.Ac

Interlayer magnetoresistance of layered conductors shows remarkable angular dependence as a function of magnetic field orientations [1]. Particularly, quasi-one-dimensional (Q1D) layered organic conductors, such as (TMTSF)₂ClO₄, where TMTSF denotes tetramethyltetraselenafulvalene, have shown very rich angular effects, the Lebed resonance [2], the Danner-Chaikin oscillations [3], the third angular effect [4], and the peak effect [3]. Although the magnetotransport shows nonclassical behaviors in some cases [5], most features including these effects have been explained as semiclassical Fermi surface topological effects [6,7]. They have been well reproduced by Boltzmann's magnetotransport theory based on electron orbital motion on Fermi surfaces [8]. By using the angular effects, we can study the ratio of band parameters.

In this Letter, we study the effect of electric field on the magnetoresistance angular effects, particularly on the Lebed resonance, in Q1D conductors. Electric fields modify the angular effects through the change of electron orbital motion. Using the electric field effect, we can obtain the information not only on the ratio between band parameters but also their absolute value.

First, we overview the semiclassical picture of magnetoresistance angular effects in Q1D multilayer systems [8]. Let us consider the simplest band model for Q1D conductors [3],

$$E(\mathbf{k}) = \hbar v_F(|k_x| - k_F) - 2t_b \cos b k_y - 2t_c \cos c k_z. \quad (1)$$

Here, orthogonal crystal axes are assumed with the x axis parallel to the conducting 1D chains and the z axis normal to the conducting 2D layers. v_F , b , and c are the Fermi velocity along the 1D chain, the interchain distance inside each layer, and the interlayer distance, respectively. The transfer energy t_c between two neighboring layers is assumed to be much smaller than the transfer energy t_b between two neighboring chains within the same layer ($t_c \ll t_b$). Such a system has a pair of sheetlike Fermi surfaces as shown in Fig. 1.

Under magnetic fields, electrons carry out orbital motions on two Fermi sheets following the equations of

motion, $\hbar \dot{\mathbf{k}} = (-e)\mathbf{v} \times \mathbf{B}$, $\mathbf{v} = (1/\hbar)\partial E(\mathbf{k})/\partial \mathbf{k}$. The interlayer conductivity $\sigma_{zz}(\omega)$ can be evaluated using the Chambers formula which sums up the contributions from all orbits [6,8]. When the interlayer transfer energy t_c is so small as to satisfy $|B_z/B_x| \gg 2t_c c/\hbar v_F$, we can easily obtain an analytic formula for $\sigma_{zz}(\omega)$.

$$\sigma_{zz}^{(0)}(\omega) = N(E_F) \left(\frac{e t_c c}{\hbar} \right)^2 \sum_{\pm, \nu} J_{\nu}^2 \left(\frac{2 t_b c}{\hbar v_F} \frac{B_x}{B_z} \right)^2 \times \frac{\tau}{1 + \left\{ \omega - v_F \left(\nu \frac{b e B_z}{\hbar} \pm \frac{c e B_y}{\hbar} \right) \right\}^2 \tau^2}. \quad (2)$$

Here, $N(E_F) = 4/(2\pi b c \hbar v_F)$ is the density of states per unit volume including spin degeneracy. τ is the scattering time, and $J_{\nu}(z)$ is the ν th Bessel function. Equation (2) corresponds to the lowest order contribution of interlayer transfer t_c to the interlayer conduction [9]. Let us note that this formula is slightly changed from that in the quantum mechanical picture [9].

Equation (2) explains most of magnetotransport features observed in Q1D conductors. dc interlayer conductivity

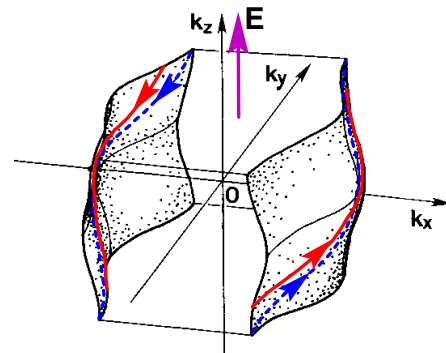


FIG. 1 (color online). Schematic sheetlike Fermi surfaces of Q1D conductors and electron orbits. Under tilted magnetic fields, electrons on different Fermi sheets move along dashed curves with the same slope. When the electric field is applied, they move along solid curves with different slopes. The deviation of electron orbits from the Fermi sheets is ignored.

$\sigma_{zz}(\omega = 0)$ shows resonant increase when $pbeB_z/\hbar \pm ceB_y/\hbar = 0$ (p is an integer). This is the Lebed resonance at the p th magic angle $B_y/B_z = p(b/c)$. In general field orientations, an electron trajectory sweeps all over the Fermi sheet, so that the interlayer velocity averaged along the orbit, $\langle v_z \rangle$, is zero. On the other hand, at the magic angles, the electron motion on the Fermi sheets becomes periodic, and averaged velocity $\langle v_z \rangle$ becomes finite causing resonant increase of interlayer conduction. The amplitude of the p th Lebed resonance, $J_p[(2t_b c/\hbar v_F)(B_x/B_z)]^2$, oscillates when the field is tilted to the 1D axis. This causes the Danner-Chaikin oscillations. The p th Lebed resonance shows a maximum peak at $(2t_b c/\hbar v_F)(B_x/B_z) \sim p$, so that all the Lebed resonance maxima satisfy $B_y/B_x = 2t_b b/\hbar v_F$. These maxima converge to a single peak of the third angular effect at the limit of $p \rightarrow \infty$. However, the peak effect cannot be deduced from the lowest order contribution represented by Eq. (2).

On the other hand, ac interlayer conductivity $\sigma_{zz}(\omega)$ shows open orbit cyclotron resonances at $\omega = v_F(pbeB_z/\hbar \pm ceB_y/\hbar)$. These resonances have been observed as the ‘‘Fermi surface traversing resonance (FTR)’’ [10] or the ‘‘periodic orbit resonances (POR)’’ [11] in microwave absorption.

Now, let us consider the effect of electric fields applied along the stacking direction. The equation of motion changes to $\hbar \mathbf{k} = (-e)\mathbf{v} \times \mathbf{B} + (-e)\mathbf{E}$. Roughly speaking, in Q1D systems with two Fermi sheets, the electric field $\mathbf{E} = (0, 0, E_z)$ tends to tilt electron open orbits as shown in Fig. 1. Here, we have to note that the electron orbits deviate from the Fermi surfaces under electric fields. However, this deviation is less than $4t_c/\hbar v_F$ in the \mathbf{k} space, so that the electron orbits can be treated to exist almost on Fermi sheets when the warping of the Fermi sheets is small.

If the warping is ignored, electrons on the $k_x > 0$ Fermi sheet have a group velocity $\mathbf{v} = (v_F, 0, 0)$, and electrons on the $k_x < 0$ sheet have $\mathbf{v} = (-v_F, 0, 0)$. In this case, the electric force $(-e)\mathbf{E}$ can be replaced by the virtual Lorentz force $(-e)\mathbf{v} \times \mathbf{B}_{\text{eff}}$, where the effective magnetic field is defined as $\mathbf{B}_{\text{eff}} = (0, E_z/v_F, 0)$ for the $k_x > 0$ Fermi sheet and as $\mathbf{B}_{\text{eff}} = (0, -E_z/v_F, 0)$ for the $k_x < 0$ sheet. Since electrons on the Fermi sheet then move as if they are under the magnetic field $\mathbf{B} + \mathbf{B}_{\text{eff}}$, the direction of electron open orbits is tilted from those in absence of electric field. The Lebed resonance condition is accordingly modified to $(B_y \pm E_z/v_F)/B_z = p(b/c)$ or

$$\frac{B_y}{B_z} = \tan\theta \sin\varphi = p \frac{b}{c} \mp \frac{E_z}{v_F B_z}. \quad (3)$$

Here, θ is the polar angle of \mathbf{B} from the z axis, and φ is the azimuthal angle of \mathbf{B} around the z axis measured from the x axis. We have to note that the Lebed resonance condition (3) is different for two Fermi sheets. In other words, under electric fields, a single Lebed resonance splits into double resonances, each of which originates from opposite Fermi sheet.

Equation (2) can be extended for finite interlayer electric fields E_z if we could employ the similar calculation as in (2). The interlayer dc current $j_z(\omega = 0)$ can be approximately represented as

$$\text{Re} \left\{ \frac{j_z(\omega = 0)}{E_z(\omega = 0)} \right\} = N(E_F) \left(\frac{et_c c}{\hbar} \right)^2 \sum_{\pm, \nu} J_\nu \left(\frac{2t_b c}{\hbar v_F} \frac{B_x}{B_z} \right)^2 \times \frac{\tau}{1 + \left\{ \omega_B - v_F \left(\nu \frac{beB_z}{\hbar} \pm \frac{ceB_y}{\hbar} \right) \right\}^2 \tau^2}. \quad (4)$$

Here, $\omega_B \equiv ceE_z/\hbar$ is the Bloch frequency. We can see that the interlayer current $j_z(\omega = 0)$ shows resonant increase when the generalized Lebed resonance condition (3) is satisfied.

Using Eq. (4), we can simulate the angular dependent interlayer conduction under electric fields. Figure 2(a) shows the ratio of interlayer current j_z and electric field E_z traced as a function of magnetic field orientation for several interlayer electric fields. The field configuration is shown in the inset of Fig. 2(a). Magnetic field with a fixed strength B is rotated in a plane including the z axis with a fixed azimuthal angle $\varphi = 60^\circ$. The parameter $\varepsilon \equiv E_z/v_F B$ indicates electric field strength. In this calculation, we have assumed a set of band parameters $a:b:c = 1.0:2.0:3.7$, $t_a:t_b:t_c = 1.0:0.1:0.003$, and $v_F = \sqrt{2}t_a a/\hbar$ so as to simulate TMTSF compounds. A relaxation time $\tau = 20/(v_F beB/\hbar)$ is employed. The ordinate j_z/E_z is normalized by the factor $N(E_F)(et_c c/\hbar)^2/(v_F beB/\hbar)$. At the limit of zero electric field ($\varepsilon \rightarrow 0$), $j_z/E_z (\rightarrow \sigma_{zz})$ shows several single-peak structures labeled by the index p corresponding to the conventional Lebed resonances. Under finite electric fields, each single peak splits to double peaks of which the width increases with the applied electric field.

Figure 2(b) shows the density plot of j_z/E_z as a function of magnetic field orientations. Darkness indicates the value

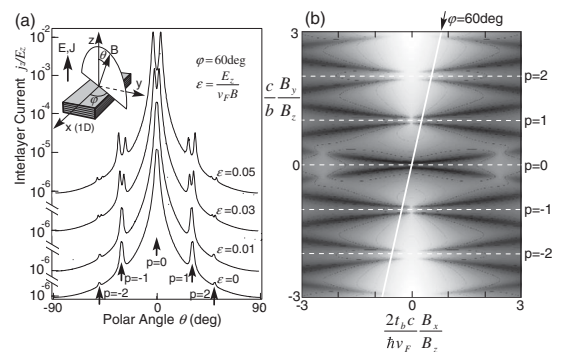


FIG. 2. Calculated interlayer conduction in Q1D conductors under the electric field as a function of magnetic field orientation. (a) Interlayer current for several electric fields when the magnetic field is rotated in a plane normal to conducting layers. (b) Angular dependent pattern of interlayer current for general magnetic field orientations.

of j_z/E_z . Here, the magnetic field strength B is assumed to be constant, and the electric field is chosen as $\varepsilon = 0.03$. The abscissa $B_x/B_z = \tan\theta \cos\varphi$ is normalized by $(2t_b c/\hbar v_F)^{-1}$ so as to be the operand of the Bessel function in Eq. (4). On the other hand, the ordinate $B_y/B_z = \tan\theta \sin\varphi$ is normalized by b/c so as to give the Lebed resonance at interger values at zero electric field as indicated by dashed horizontal lines. Under the electric field, each Lebed resonance splits into two branches obeying (3), which appear as a pair of dark hyperbola in the figure. The amplitude of each branch, that is, the darkness of each hyperbola, is modulated as B_x/B_z is changed..

The tilted white line indicates the trace of magnetic field rotation with fixed B and φ , which corresponds to the experimental scan as simulated in Fig. 2(a). When a Lebed resonance splits into double peaks at θ_+ and θ_- in the field rotation, the difference $\Delta \tan\theta \equiv |\tan\theta_+ - \tan\theta_-|$ satisfies the following relation,

$$\Delta \tan\theta = \frac{2V}{dv_F B \sin\varphi} \sqrt{1 + \tan^2\theta}. \quad (5)$$

Here, d and $V = E_z d$ are the sample thickness and the applied voltage along stacking direction, respectively. In the right-hand side, $\tan\theta$ means the center position of double peaks $(\tan\theta_+ + \tan\theta_-)/2$. Since B , V , d , and φ can be measured, we can experimentally determine the Fermi velocity v_F from the split of the Lebed resonance.

Another experimental method to determine the Fermi velocity v_F in Q1D conductors uses the POR in microwave absorption measurement [11]. The present method using just dc transport gives the same information as POR since Eq. (4) is obtained by substituting the Bloch frequency ω_B for the microwave frequency ω in Eq. (2).

In order to demonstrate the above electric field effect in real systems, we have performed angular magnetotransport measurements of layered organic conductors under pulsed high electric fields. First, we chose one of the most typical Q1D organic conductors $(\text{TMTSF})_2\text{ClO}_4$, where all of magnetoresistance angular effects in Q1D systems have been well established. Although we observed unclear shift of Lebed resonances, we could not see clear splitting [12]. In the case of $(\text{TMTSF})_2\text{ClO}_4$, interlayer resistivity is too small to apply high electric fields. Too much current easily heats up electron temperature and blurs out the splitting. Then, we selected the organic conductor $\alpha\text{-(BEDT-TTF)}_2\text{KHg(SCN)}_4$, where BEDT-TTF denotes bis(ethylenedithia-tetrathiafulvalene). This layered compound has thick polymeric insulating layers so that it shows large interlayer resistivity compared to $(\text{TMTSF})_2\text{ClO}_4$.

It has been known that $\alpha\text{-(BEDT-TTF)}_2\text{KHg(SCN)}_4$ undergoes a phase transition to the charge-density-wave (CDW) phase at about 10 K [13]. Clear observation of Lebed resonances [14,15] and POR (or FTR) [10,11] in this CDW phase strongly suggests that sheetlike Fermi surfaces exist in the electronic structure reconstructed by CDW formation [16,17]. The Lebed resonances appear at mag-

netic field orientations satisfying $\tan\theta = (1.27p - 0.55)/\cos(\phi - \phi_0)$, where θ and ϕ are the polar angle from the crystal \mathbf{b}^* axis (normal to the conducting ac plane) and the azimuthal angle around the \mathbf{b}^* axis measured from the \mathbf{a} axis, respectively [15]. p is an integer, and $\phi_0 = 27^\circ$. This fact shows that the 1D axis normal to the Fermi sheets is tilted by $\phi_0 - \pi/2 = -63^\circ$ from the \mathbf{a} axis in the ac plane in the CDW phase.

Single crystals of $\alpha\text{-(BEDT-TTF)}_2\text{KHg(SCN)}_4$ have been grown by the conventional electrochemical method. The interlayer conduction under strong electric fields was measured using pulsed electric fields to avoid sample heating. Electric contacts were formed by gold evaporation on the top and bottom flat surfaces. Typical crystal thickness is $d = 0.1\text{--}0.2$ mm. Pulsed voltage V was applied between the top and bottom surfaces, and the responding interlayer current was measured. The waveforms of both voltage and current pulses were recorded in the 12-bit digitizer. The pulse width of $5 \mu\text{s}$ and the duty ratio of $1/3000$ were chosen so as to avoid sample heating. Although the measured voltage-current characteristics were nonlinear, they showed no clear threshold behavior for the sliding motion of CDW. The samples were mounted on the rotating holder with 0.1° resolution, set in the 13 T superconducting magnet.

Figure 3 shows the interlayer current as a function of magnetic field orientations for several interlayer voltages. The magnetic field strength was fixed at 13 T, and the temperature was held at 1.8 K so that the system was in the CDW phase. When the interlayer voltage is low enough, for example, $V = 2$ V, the interlayer current shows a series of peaks due to the Lebed resonance as

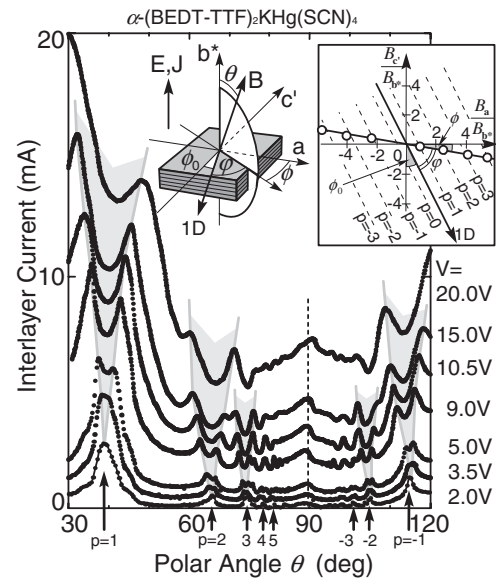


FIG. 3. Angular dependence of interlayer current for several voltages when the magnetic field is rotated in a plane normal to conducting layers in $\alpha\text{-(BEDT-TTF)}_2\text{KHg(SCN)}_4$. Inset: the observed Lebed resonance positions and the 1D axis direction of the electronic system.

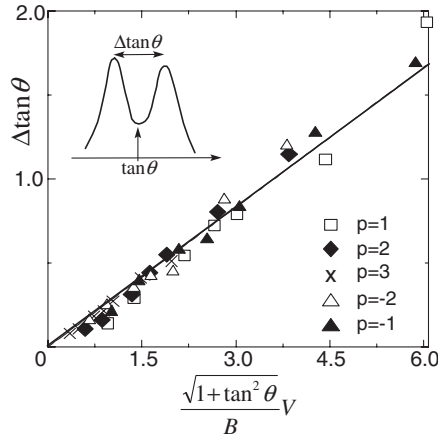


FIG. 4. Plot of split width vs normalized voltage for five Lebed resonances. The solid line indicates a fit to Eq. (5).

indicated by arrows. As shown in the inset of Fig. 3, their positions satisfy the resonance condition $\tan\theta = (1.27p - 0.55)/\cos(\phi - \phi_0)$ represented by tilted dashed lines, if we assume that magnetic fields were rotated in a plane normal to the ac plane with the fixed azimuthal angle $\phi = -9^\circ$ measured from the \mathbf{a} axis. In other words, the rotation plane was tilted by $\varphi = 54^\circ$ from the 1D axis.

At large interlayer electric fields, the Lebed resonance peaks clearly split into double peaks, and their split width increases as the applied electric field is increased. The split width becomes smaller at Lebed resonances with higher indices p . Experimental results in Fig. 3 qualitatively reproduce those of Fig. 2(a) calculated for an ideal Q1D system (1).

In Fig. 4, the split width is plotted as a function of the voltage for several Lebed resonances. The abscissa is normalized by the normal component of magnetic field $B_z = B(1 + \tan^2\theta)^{-1/2}$. Here, the split width and the center position are determined by $\Delta \tan\theta = |\tan\theta_+ - \tan\theta_-|$ and $\tan\theta = (\tan\theta_+ + \tan\theta_-)/2$, where θ_+ and θ_- are positions of split double peaks. We can see that the split width $\Delta \tan\theta$ for different Lebed resonances with different indices p almost exist along a common straight line passing through the origin. This means that the split width is proportional to the electric field E_z and scaled by the normal component of the magnetic field as expected in Eq. (5). Therefore, we could conclude that the observed split originates from the electric field effect discussed above. From the slope of the line in Fig. 4, which is equal to $2/dv_F \sin\varphi$, we can estimate the Fermi velocity v_F as $(9.0 \pm 1.5) \times 10^4$ m/s using $d = 0.1$ mm and $\varphi = 54^\circ$. It is agreeable with the value 6.5×10^4 m/s obtained from the POR measurements [11].

In summary, we have discussed the Lebed resonance of interlayer conduction in Q1D layered conductors under strong electric fields. Under strong electric fields, two Fermi sheets show the Lebed resonances at different field orientations, of which the difference can be used to esti-

mate the Fermi velocity. We have experimentally demonstrated the above features with the low-dimensional organic conductor α -(BEDT-TTF)₂KHg(SCN)₄.

The authors are grateful to Professor M. J. Naughton for valuable suggestion on the pulse measurement. They greatly thank Professor K. Kanoda and Dr. K. Miyagawa for teaching us crystal growth. They also thank Professor W. Kang for critical reading. This work is supported by the Grant-in-Aid for Scientific Research (B) (No. 12440083 and No. 15073206) from Japan Society for the Promotion of Science and the Toray Science Foundation.

*Present address: Aoyama Gakuin University, Fuchinobe, Sagamihara 229-8558, Japan.

- [1] T. Ishiguro, K. Yamaji, and G. Saito, *Organic Superconductors* (Springer, New York, 1997), 2nd ed.
- [2] T. Osada, A. Kawasumi, S. Kagoshima, N. Miura, and G. Saito, Phys. Rev. Lett. **66**, 1525 (1991); M.J. Naughton, O.H. Chung, M. Chaparala, X. Bu, and P. Coppens, *ibid.* **67**, 3712 (1991).
- [3] G.M. Danner, W. Kang, and P.M. Chaikin, Phys. Rev. Lett. **72**, 3714 (1994).
- [4] H. Yoshino *et al.*, J. Phys. Soc. Jpn. **64**, 2307 (1995); T. Osada, S. Kagoshima, and N. Miura, Phys. Rev. Lett. **77**, 5261 (1996).
- [5] S.P. Strong, D.G. Clarke, and P.W. Anderson, Phys. Rev. Lett. **73**, 1007 (1994); G.M. Danner and P.M. Chaikin, *ibid.* **75**, 4690 (1995).
- [6] K. Maki, Phys. Rev. B **45**, R5111 (1992); T. Osada, S. Kagoshima, and N. Miura, *ibid.* **46**, 1812 (1992).
- [7] A.G. Lebed and N.N. Bagmet, Phys. Rev. B **55**, R8654 (1997).
- [8] T. Osada, N. Kami, R. Kondo, and S. Kagoshima, Synth. Met. **103**, 2024 (1999).
- [9] T. Osada and M. Kuraguchi, Synth. Met. **133-134**, 75 (2003); T. Osada, K. Kobayashi, and E. Ohmichi (to be published).
- [10] A. Ardavan, J.M. Schrama, S.J. Blundell, J. Singleton, W. Hayes, M. Kurmoo, P. Day, and P. Goy, Phys. Rev. Lett. **81**, 713 (1998).
- [11] A.E. Kovalev, S. Hill, and J.S. Qualls, Phys. Rev. B **66**, 134513 (2002).
- [12] K. Kobayashi, E. Ohmichi, and T. Osada, Synth. Met. **133-134**, 71 (2003).
- [13] P. Foury-Leykian, S. Ravy, J.-P. Pouget, and H. Muller, Synth. Met. **137**, 1271 (2003).
- [14] M.V. Kartsovnik, A.E. Kovalev, V.N. Laukhin, and S.I. Pesotskii, J. Phys. I (France) **2**, 223 (1992).
- [15] Y. Iye, R. Yagi, N. Hanasaki, S. Kagoshima, H. Mori, H. Fujimoto, and G. Saito, J. Phys. Soc. Jpn. **63**, 674 (1994).
- [16] M.V. Kartsovnik, A.E. Kovalev, and N.D. Kushch, J. Phys. I (France) **3**, 1187 (1993).
- [17] N. Harrison, E. Rzepniewski, J. Singleton, P.J. Gee, M.M. Honold, P. Day, and M. Kurmoo, J. Phys. Condens. Matter **11**, 7227 (1999).